Quantum chemical density functional theory studies on the molecular structure and vibrational   spectra of 4-amino-3-(4-chlorophenyl)-butanoic acid

T.Jayaprakash[1], K.Parimala Gandhi[2], G.Chinnasamy[3], K.Saranya[4], R.Sathishkumar[5] J. Ashok[6] and M. Jeganathan[7]

[1-5]Department of Science and Humanities, Nehru Institute of Technology, Coimbatore.

[6]Dean, Dhanalakshmi srinivasan School of Architecture, Perambalur - 621113.

[7]Associate Professor, Designed Environment and Research Institute (DEAR Institute) Trichy- 621 213.

nitparimalagandhi@nehrucolleges.com

Abstract- 4-amino-3-(4-chlorophenyl)-butanoic acid(4ACBA) otherwise commonly called as Baclofen is a drug used for the treatment of alcohol dependence The solid phase FT-IR and FT-Raman spectra of 4ACBA were recorded in the regions 4000–400 cm^{-1} and 3500–100 cm^{-1} respectively. Theoretical vibrational frequencies, geometric parameters (bond lengths and bond angles), thermodynamic properties,frequency and intensity of the vibrational bands, Natural population analysis and Mulliken atomic charges of 4ACBA were obtained by the Restricted Hartree–Fock (RHF) and density functional theory (DFT) using 6-31G(d,p) basis set. The harmonic vibrational frequencies for 4ACBA were calculated values have been compared with experimental values of FTIR and FT-Raman spectra. The observed and the calculated frequencies are found to be in good agreement. Stability of the molecule arising from hyperconjugative interactions and charge delocalization has been analyzed using natural bond orbital (NBO) analysis. The electronic dipole moment (lD) and the first hyperpolarizability (β_{tot}) values of the investigated molecule were computed using HF and (DFT/B3LYP) with 6-31G+(d,p) basis sets.The calculated results also show that the (4ACBA) molecule may have microscopy nonlinear optical (NLO) behavior with non zero values. ^{1}H and ^{13}C NMR spectra were recorded and chemical shift of the molecule were calculated using the gauge independent atomic orbital (GIAO) method.

Keywords: FTIR; FT-RAMAN; NBO; DFT

1.   Introduction

Alcoholism is a primary, chronic disease with genetic, psychosocial, and environmental factors influencing its development and manifestations. The disease is often progressive and fatal. It is characterized by impaired control over drinking, preoccupation with the drug alcohol, use of alcohol despite adverse consequences, and distortions in thinking, most notably denial. Each of these symptoms may be continuous or periodic." This definition recognizes alcoholism as a disease, i.e., as

an involuntary disability. It accepts a genetic vulnerability in some people and identifies the phenomenon of denial as both a psychological defense mechanism and a physiological outcome of alcohol's effect on the memory.It is medically considered a disease, specifically an addictive illness, and in psychiatry several other terms are used, specifically "alcohol abuse" and "alcohol dependence," which have slightly different definitions[1]. Identifying alcoholism is difficult for the individual afflicted because of the social stigma associated with the disease that causes people with alcoholism to avoid diagnosis and treatment for fear of shame or social consequences. The evaluation responses to a group of standardized questioning are a common method for diagnosing alcoholism. These can be used to identify harmful drinking patterns, including alcoholism [2].Baclofen (brand names Kemstro, Lioresal, Liofen, Gablofen, Lyflex, Beklo and Baclosan) is a derivative ofgamma-aminobutyric acid (GABA). It is primarily used to treat spasticity and is in the early research stages for use for the treatment of alcoholism. It is also used by compounding pharmacies in topical pain creams as a muscle relaxant.It is an agonist for the GABAB receptors[3,4]. Its beneficial effects in spasticity result from actions at spinal andsupraspinal sites. Baclofen can also be used to treat hiccups, and has been shown to prevent rises in body temperature induced by the drug MDMA in rats[5].Baclofen is also used to treat muscle spasms caused by certain conditions (such as multiple sclerosis, spinal cord injury/disease). It works by helping to relax the muscles. Converging evidence suggest that the gamma-aminobutyric acid-B receptor agonist baclofen is a promising agent for the treatment of alcoholism. Baclofen side effects include drowsiness, weakness, dizziness, headache, seizures, nausea, vomiting, low blood pressure, constipation, confusion, respiratory depression, insomnia, and increased urinary frequency or urinary retention. Abrupt discontinuation of baclofen may cause seizures and hallucinations, high fever, rebound spasticity, muscle rigidity, and rhabdomyolysis. Baclofen is a white (or off white) mostly odorless crystalline powder, with a molecular weight of 213.66 g/mol. It is slightly soluble in water, very slightly soluble inmethanol, and insoluble in chloroform. Baclofen Tablets USP 10 mg and 20 mg contain the following inactive ingredients: magnesiumstearate, microcrystalline cellulose, povidone and starch (corn).It is manufactured by LANNETT COMPANY, INC.Philadelphia, PA 19136 Made in the USA. (Vasanthy and Jeganathan 2007, Vasanthy et.al., 2008, Raajasubramanian et.al., 2011, Jeganathan et.al., 2012, 2014, Sridhar et.al., 2012, Gunaselvi et.al., 2014,Premalatha et.al., 2015, Seshadri et.al., 2015, Shakila et.al., 2015, Ashok et.al., 2016, Satheesh Kumar et.al., 2016).

2. Experimental details

The pure compound 4ACBA was purchased from USA with more than 98% purity and was used as such without further purification to record FTIR and FT Raman spectra.The FTIR spectrum of the compound is recorded in the region 4000–400 cm^{-1} in evacuation mode on Bruker IFS 66V spectrophotometer using KBr pellet technique (solid phase) with 4.0 cm^{-1} resolution. The FT Raman spectrum is recorded using 1064 nm line of Nd:YAG laser as excitation wavelength in the region 3500–100 cm^{-1}on Bruker IFS 66V spectrometer equipped with FRA 106 FT Raman module accessory. The spectral measurements were carried out at Sophisticated Instrumentation Analysis Facility, IIT,Madras, India. The experimental FTIR and FT Raman spectra of CAS are presented in the Figs.1and 2.
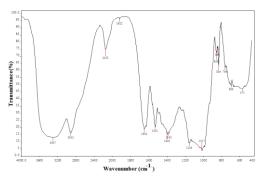

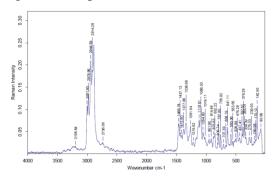
Fig.1. FTIR spectrum of 4ACBA molecule

Fig.2. FTRAMAN spectrum of 4ACBA molecule

3. Computational methods

In the present work, the density functional method (DFT) [6] has been employed using Becke's three parameter hybrid exchange functional with the Lee–Yang–Parr correlation functional [7,8] to optimize the structure of the molecule and also to calculate the electronic structure of the title molecule. The entire calculations were performed at ab initio HartreeFock (HF) and DFT method using B3LYP levels at 6-31G(d,p) basis sets on a Pentium V/1.6 GHz personal computer by using Gaussian 03 W program package [9,10] and applied geometry optimization [11]. Initial geometry generated, was minimized at the HartreeFock level using 6-31 G(d,p) basis set and also optimized at DFT/B3LYP levels at 6-31G(d,p) basis set. The vibrational modes are assigned using Gauss-View

molecular visualization program package. The optimized structural parameters were used in the vibrational frequency calculations at the DFT levels to characterize all stationary points as minima. The vibrational frequencies were calculated and scaled down by the appropriate scaling factor and thereby the vibrational assignments are compared with observed values. Furthermore, in order to show nonlinear optics (NLO) activity of title molecule, the dipole moment, linear polarizability and first hyper polarizability were obtained. The natural bonding orbital (NBO) calculations [12] were performed using NBO 3.1 program as implemented in the Gaussian 03W package at the above said level in order to understand various second order interactions between the filled orbital of one subsystem and vacant orbital of another subsystem, which is a measure of the intermolecular and intramolecular delocalization or hyper conjugation. The molecular geometry was not restricted and all the calculations (vibrational wave numbers,geometric parameters and other molecular properties) were performed by using Gauss View molecular visualization program [13] and Gaussian 03 program package on a computing system [14]. (Manikandan et.al., 2016, Sethuraman et.al., 2016, Senthil Thambi et.al., 2016).

4.   Results and discussion

4.1   Molecular geometry

The optimized structure parameters of 4ACBA is calculated by DFT and HF level with 6-31G(d,p) basis set shown in Table.1in accordance with the atom numbering scheme given in Fig.3 The comparative optimized structural parameters such as bond length, bond angle along with its experimental data's are presented in Table.1. The molecule has 26 atoms and 72 normal modes of fundamental vibrations. All the 72 vibrations are active in both IR and Raman.A general priority for reproducing the experimental bond lengths and bond angles [15] is not present among HF and DFT levels. All calculated geometrical parameters obtained at the DFT level of theory are in good agreement with the experimental structural parameters. The molecule has 10 C-C bond lengths, 2 C-O and N-H bond lengths, nine C-H bond lengths, one C-N,O-H,C-CL bond lengths. The C-C bond lengths in the optimized geometry of 4ACBAcalculated at both levels fall in the range; 1.394–1.515 Å.It is close agreement with the experimental values [16]. A similar trend has also been observed in the case of the C-N, O-H,C-CL bonds. The nine C-H lengths (1.113 Å) are almost equal at B3LYP/6-31+G(d,p) basis set.From theoretical values, we found most of the optimized bond lengths are in good agreement with experimental bonds lengths, but bond angles are slightly longer and shorter than that of experimental values.

4.2   Vibrational assignments

IR and Raman spectra contain a number of bands at specific wavenumbers. The aim of the vibrational analysis is to decide which of the vibrational modes give rise to each of these observed bands. According to the theoretical calculations, 4ACBA has a structure of C_1 point groupsymmetry.The molecule has 26 atoms and 72 normal modes of fundamental vibrations (3N-6).A satisfactory vibrational band assignment has been done.Almost all the 72 fundamental vibrations are active in both IR absorption and Raman scattering.The frequencies of fundamental vibrational modes together with intensities calculated on the basis of HF and DFT methods are tabulated in Table 2.Chemcraft [17], a graphical interface, was used to assign the calculated harmonic wavenumbers using scaled displacement vectors to identify the motion of modes.On the whole, the predicted vibrational wavenumbers are in agreement with the experimental results.

C–NH$_2$ vibrations

The molecule under investigation possesses only one NH2 group and hence one expects one symmetric and one asymmetric N– H stretching vibrations in NH2group. In all the primary aromatic amines, the N–H stretching frequency occurs in the region $3300–3500 cm^{-1}$[18]. The asymmetric-NH2 stretching vibration appears from 3500 to 3420 cm^{-1} and the symmetric- NH2 stretching is observed in the range 3420– 3340 cm^{-1} [19].Hence, the band in IR spectrum were located at 3307 cm^{-1} and Raman spectrum were located at 3275 cm^{-1} are assigned to N–H symmetric and asymmetric stretching vibrations, respectively in NH2 group. These assignments agree well with the earlier reports[20].The scaled NH2 symmetric and asymmetric stretching are in the range of $3308–3278 cm^{-1}$ in B3LYP/6-31+G(d,p).The various vibrations NH2group of the title compound are also found to be in good agreement with the experimental values.

C-H vibration

The existence of one or more aromatic rings in a structure is normally readily determined from the C-H and C-C ring related vibrations. The substituted benzene like molecule gives rise toC-H stretching, C-H in-plane and C-H out-of-plane bending vibrations. The hetro aromatic structure shows the presence of C-H stretching vibration in the region $3100–3000 cm^{-1}$, which is the characteristic region for the ready identification of C-H stretching vibration [21,22]. In this region, the bands are not affected appreciably by the nature of the substituent. The aromatic C-H stretching frequencies arise from the modes observed at 3062, 3047 cm^{-1} and 3080 cm^{-1} of benzene and its derivatives [23]. In our present work, the C-H stretching vibrations are observed at 2907 cm^{-1} in FT-Raman spectrum for C-H vibrations. The calculated values of these modes for the title molecule have been found to be 2820 cm^{-1} and 2911 cm^{-1} at HF and B3LYP calculation level. In general the

aromatic C–H stretching vibrations calculated theoretically are in good agreement with the experimentally values.

C–C vibrations

The carbon–carbon stretching modes of the phenyl group are expected in the range from 1650 to 1200 cm^{-1}. The actual position of these modes is determined not so much by the nature of the substituent but by the form of substitution around the ring [24]. In general, the bands are of variable intensity and are observed at 1625–1590, 1590–1575, 1540–1470, 1465–1430 and 1380– 1280 cm^{-1} from the frequency ranges given by Varsanyi [25] for the five bands in the region. In the present work, the wave numbers observed in the FTIR spectrum at 1489,1400 cm^{-1} and FT-Raman spectrum 1460,1437,1413 cm^{-1} have been assigned to C-C stretching vibrations.

CH$_2$ vibrations

For the assignments of CH$_2$ group frequencies, basically six fundamentals can be associated to each CH2 group namely CH$_2$ symmetric stretch; CH$_2$asymmetric stretch; CH$_2$ scissoring and CH$_2$ rocking which belongs to in plane vibrations and two out-of-plane vibrations, viz., CH$_2$ wagging and CH$_2$ twisting modes, which are expected to be polarized [26]. The asymmetrical CH$_2$ stretching vibrations are generally observed around 3000 cm^{-1} while the symmetric stretch will appear between 3000 and 2900 cm^{-1} region [27,28]. In this study, the asymmetric stretching vibrations are observed at 2975 cm^{-1} in FTIR and 2978 cm^{-1} in FT-Raman spectrum and symmetric stretching vibrations are observed at 2928,2912 cm^{-1} in FTIR and 3198,3063 cm^{-1} in the FT-Raman spectrum .These experimental values correlates well with the HF and B3LYP calculation level .

Deformation vibrations

The C-C-C bending bands always occur below 700 cm^{-1}.Isopropyl benzenes [29,30] have a medium intensity absorption band in the region 545-525 cm$^{-1.}$.The C-C-C vibration is found at 671 cm^{-1} in the FT-IR spectrum and 668 cm^{-1} in the FT-Raman spectrum.This correlates well with the calculated values.

4.6   Natural population analysis

Population analysis is the study of charge distribution within molecules.The calculation of effective atomic charges plays an important role in the application of quantum mechanical calculations to molecular systems [31].Our interest here is in the comparison of different methods (RHF and DFT) to describe the electron distribution in 4ACBA is broadly as possible, and to assess the sensitivity of the calculated charges to changes in the choice of the quantum chemical method. The calculated atomic charge values from the natural population analysis (NPA) and Mulliken

population analysis (MPA) procedures using the RHF and DFT methods are listed in Table 3. The charge distribution of 4ACBA is shown in Fig.4. The NPA from the natural bonding orbital (NBO) method is better than the MPA scheme. The NPA of 4ACBA shows the presence of Nitrogen atoms in the hydrogen moiety [N_6= -0.95433(DFT) and N_6= -0.99946(RHF)] imposes positive charges on the hydrogen atoms H_{25}=0.40392(DFT), H_{25}=0.40987(RHF) and H_{26}= 0.40375(DFT), H_{26}= 0.41061(RHF). However the oxygen atom O_6 possess large negative charges, resulting in the positive charges on the C_1 and H_{20} atoms.Moreover, there is no differences in charge distribution observed on all hydrogen atoms except the H_{20},H_{25},H_{26} Hydrogen atoms. The large positive charge on these hydrogen atoms is due to the large negative charge accumulated on the N_{14} and O_6 atoms respectively.

4.7   Thermodynamic properties

Several calculated thermodynamic parameters such as,rotational constants, zero point thermal energy, specific heat capacity,entropy,dipole moment,Gibbs free energy have been presented in Table 4.Scale factors have been recommended [32] for accurate reductions in determining the Zero-Point Vibration Energies (ZPVEs) and the entropy, the variations in the PVEs seem to be significant. The total energies and the change in the total entropy of 4ACBA at room temperature by different methods are also presented in Table 4.The change in the Gibbs free energy of 4ACBA at room temperature for both the methods are only marginal.The highest value of ZPVE of 4ACBA is 140.634 kcal mol^{-1} obtained by HF/6-31+G(d,p), whereas the lowest one is 130.955 kcal mol^{-1}, obtained by B3LYP/6-31+G(d,p) method. Dipole moment reflects the molecular charge distribution and is given as a vector in three dimensions. Therefore, it can be used as an illustrator to depict the charge movement across the molecule. As a result, the dipole moment of 4ACBA was observed at 2.3931D in HF/6-31+G(d,p) method whereas 3.4111D in B3LYP/6-31+G(d,p)method.

4.8   NLO properties

The first hyperpolarizability (β_0) of this novel molecular system and related properties (β_{tot}, α, $\Delta\alpha$) of 4ACBA are calculated using DFT/B3LYP methods at 6-31+G(d,p) basis set based on the finite field approach. In the presence of an applied electric field, the energy of a system is a function of the electric field. First, hyperpolarizability is a third-rank tensor that can be described by a 3x 3 x 3 matrix. The 27 components of the 3D matrix can be reduced to 10 components due to the Kleinman symmetry [33]. It can be given in the lower tetrahedral format. It is obvious that the lower part of the 3x 3 x 3 matrixes is a tetrahedral. The components of β are defined as the coefficients in the Taylor

series expansion of the energy in the external electric field. When the external electric field is weak and homogeneous, the expansion becomes

$$E = E^0 - \mu_x F_\alpha - 1/2\alpha_{\alpha\beta} F_\alpha F_\beta - 1/6\beta_{\alpha\beta\gamma}F_\alpha F_\beta F_\gamma + \ldots\ldots(1)$$

where E^0 is the energy of the unperturbed molecules, F_α is the field at the origin and μ_x, $\alpha_{\alpha\beta}$ and $\beta_{\alpha\beta\gamma}$ are the components of dipole moment, polarizability and the first hyperpolarizabilities respectively. The total static dipole moment μ_D, the mean polarizabilityα, the anisotropy of the polarizability $\Delta\alpha$ and the mean first hyperpolarizabilityβ_{tot} using the x, y, z components, they are defined as

$$\mu_D = (\mu^2_x + \mu^2_y + \mu^2_z)^{1/2}$$

$$\alpha = \frac{\alpha_{xx} + \alpha_{yy} + \alpha_{zz}}{3}$$

$$\Delta\alpha = 2^{-1/2} [(\alpha_{xx} - \alpha_{yy})^2 + (\alpha_{yy} - \alpha_{zz})^2 + (\alpha_{zz} - \alpha_{xx})^2 + 6 \alpha^2 xx]^{1/2}$$

$$\beta_{tot} = (\beta^2_x + \beta^2_y + \beta^2_z)^{1/2} \text{ and}$$

$$\beta_x = \beta_{xxx} + \beta_{xyy} + \beta_{xzz}$$

$$\beta_y = \beta_{yyy} + \beta_{xxy} + \beta_{yzz}$$

$$\beta_z = \beta_{zzz} + \beta_{xxz} + \beta_{yyz}$$

The calculation of the total molecular dipole moment (μ_D), linear polarizability (α) and first hyperpolarizability (β_{tot}) from the Gaussian output have been explained in detail previously [34],and DFT has been extensively used as an effective method to investigate the organic NLO materials [35–39]. In addition, the polar properties and dipole moment of the title compound were calculated at the B3LYP/6-31+G(d,p) level using Gaussian 03W program package.

$$E = E^0 - \mu_x F_\alpha - 1/2\alpha_{\alpha\beta} F_\alpha F_\beta - 1/6\beta_{\alpha\beta\gamma}F_\alpha F_\beta F_\gamma + \ldots\ldots$$

where E^0 is the energy of the unperturbed molecules, F_α is the field at the origin and μ_x, $\alpha_{\alpha\beta}$ and $\beta_{\alpha\beta\gamma}$ are the components of dipole moment, polarizability and the first hyperpolarizabilities respectively. The total static dipole moment μ_D, the mean polarizabilityα, the anisotropy of the polarizability $\Delta\alpha$ and the mean first hyperpolarizabilityβ_{tot} using the x, y, z components, they are defined as

$$\mu_D = (\mu^2_x + \mu^2_y + \mu^2_z)^{1/2}$$

$$\alpha = \alpha_{xx} + \alpha_{yy} + \alpha_{zz}$$

—— $\overline{3}$ ——

$$\Delta\alpha = 2^{-1/2} [(\alpha_{xx} - \alpha_{yy})^2 + (\alpha_{yy} - \alpha_{zz})^2 + (\alpha_{zz} - \alpha_{xx})^2 + 6\,\alpha^2 xx]^{1/2}$$

$$\beta_{tot} = (\beta^2_x + \beta^2_y + \beta^2_z)^{1/2} \text{ and}$$

$$\beta_x = \beta_{xxx} + \beta_{xyy} + \beta_{xzz}$$

$$\beta_y = \beta_{yyy} + \beta_{xxy} + \beta_{yzz}$$

$$\beta_z = \beta_{zzz} + \beta_{xxz} + \beta_{yyz}$$

The calculation of the total molecular dipole moment (μ_D), linear polarizability (α) and first hyperpolarizability (β_{tot}) from the Gaussian output have been explained in detail previously,and DFT has been extensively used as an effective method to investigate the organic NLO materials. In addition, the polar properties and dipole moment of the title compound were calculated at the B3LYP/6-31G (d,p) level using Gaussian 03W program package.

Urea is one of the prototypical molecules used is the study of the NLO properties of the molecular systems. Therefore it was used frequently as a threshold value for comparative purposes. The calculated dipole moment and hyperpolarizability values obtained from B3LYP/6-31G method are collected in Table 5.The total molecular dipole moment of 4ACBA from B3LYP with 6-31+G (d,p) basis set is 7.9313D which is five times greater than the value for urea ($\mu_D = 1.3732D$). Similarly the first order hyperpolarizability of 4ACBA with B3LYP/6-31+G(d,p) basis set is 3.0539 x 10^{-30}esu which is greater than the value of urea ($\beta_{tot} = 0.372 \times 10^{-30}$esu). From the computation the high values of the hyperpolarizability of 4ACBA are probably attributed to the charge transfer existing between the phenyl rings within the molecular skeleton. This is evidence for nonlinear optical (NLO) property of the molecule.

4.9.   NBO Analysis

Some electron donor orbital, accepter orbital and the interacting stabilization energy resulting from the second- order micro-disturbance theory is reported [40,41]. The larger the stabilization energy value, the more intensive is the interaction between electron donors and electron accepters, i.e. the more donating tendency from electron donors to electron accepters and the grater the extent of conjugation of the whole system. Delocalization of electron density between occupied Lewis-type (bond or lone pair) NBO orbitals and formally unoccupied (anti-bond or Rydberg) non-Lewis NBO orbitals corresponds to a stabilizing donor– accepter interaction. The intramolecular interaction are formed by the orbital overlap between (C–C), *(C–C), (N– C),*(N–C), (C–C), –*(C–C) bond orbital

which results intramolecular charge transfer (ICT) causing stabilization of the system. These interactions are observed as increase in electron density (ED) in C– C anti bonding orbital that weakens the respective bonds. These intramolecular charge transfer (σ—σ^*, π –π^*) can induce large nonlinearity of the molecule.

The strong intramolecular hyper conjugation interaction of the r and p electrons of C–C, N–C and C–O to the anti C–C, C–H, N–C and C–O bonds leads to stabilization of some part of the ring as evident from Table 6. NBO analysis has been performed on the molecule at the B3LYP/6-31G (d,p) level in order to elucidate the intramolecular, re-hybridization and delocalization of electron density within the molecule.For example the intramolecular hyperconjugative interaction of σ (C7–C12) distribute to σ^*(C1-C2),(C2-C3),(C3-C4),(C8-C9),(C10-C11) leading to stabilization of 22.76kJ/mol.NBO analysis clearly manifests the evidences of the intra-molecular charge transfer from π (C8–C9) to π^*(C7–12) anti-bonding Orbital's as shown in Table 6, that clearly shows stabilization energy of 21.07kJ/mol. The same leads to a strong stabilization energy of 20.56kJ/mol of (C10–C11).

4.10   NMR - ^{1}H and ^{13}Cspectral analysis

The isotropic chemical shifts are frequently used as an aid in the identification of reactive organic as well as ionic species.It is recognized that accurate predictions of molecular geometries are essential for reliable calculations of magnetic properties.^{1}H and ^{13}C chemical shift calculations of the compound have been made by same method GIAO [42]procedure is somewhat superior since it exhibits a faster concern of the calculated properties upon extension of the basis set used and ^{1}H and ^{13}C NMR spectra as shown in Fig.5.Taking in account the computational cost and the effectiveness of calculation,the GIAO method seems to be preferable from many aspects at the present state,the density functional methodologies offer an effective alternative to the conventional correlated methods, due to their significantly lower computational cost.The ^{1}H and ^{13}C chemical shifts are measured in a less polar (DMSO) solvent.The results in Table7shows the range ^{13}CNMR chemical shift of the typical organic molecule usually is > 100 [43] the accuracy ensures reliable interpretation of spectroscopic parameters. The ^{13}CNMR chemical shift of C_1 and C_7 are observed larger than carbons whereas their chemical shifts are lower than all other observed.This C_3 and C_4 chemical shifts are determined at 169.324 and 141.895 ppm for 4ACBA.The protons of 4ACBA are observed at 9.149 for H_{21} and at 8.211 for H_{22} ppm respectively.

Another important aspect is that hydrogen attached or nearby an electron withdrawing atom or group can decrease the shielding and move the resonance of attached proton towards to higher

frequency.By contrast electron donating atom or group increases the shielding and moves the resonance towards to a lower frequency.Electronegative atoms such as nitrogen,oxygen and halogens deshielded hydrogens. The extent deshielding is proportional to the electronegativity of the hetero atom and its proximity to the hydrogen.Electrons on an aromatic ring, double bonded atoms, and triple bonded atoms deshield attached hydrogens.The two oxygen atoms of 4ACBA show electronegative property. The presence of electronegative atom attracts all electron clouds of carbon atoms towards them of carbon atom and net result is increase in chemical shift.   .Also the chemical shifts obtained and calculated for the hydrogen atoms are quite low are due to shielding effect.The oxygen atoms i.e more electronegative property polarizes the electron distribution in its bond and decreases the electron density of the compounds.

5.   Conclusion

The investigation of the present work, the compute vibrational and molecular structure analysis has been performed based on the quantum mechanical approach by B3LYP/6-31G+(d,p) and HF/6-31G(d,p) calculations. On the basis of the calculated and experimental results assignment of the fundamental frequencies were examined. The available experimental results were compared with theoretical data. The optimized geometry is tabulated in comparison with the experimental XRD data and well discussed. The electric dipole moment, polarizabilities and the hyperpolarizabilities of the compound studied that have been calculated by B3LYP/6-31G(d,p) and HF/6-31G(d,p) method. NLO properties of the 4ACBA aniline are much greater than those of urea. NBO analysis was made and it is indicating the intramolecular charge transfer between the bonding and antibonding orbitals. Orbital energy interactions between selective functional groups were analyzed by density of energy states. The Mulliken charges and natural atomic charges of the title molecule have been studied by both the HF and DFT methods. The calculated normal-mode vibrational frequencies provide thermodynamic properties by the way of statistical mechanics. Theoretical ^{1}H and ^{13}C chemical shift values were reported and compared with experimental data, showing good agreement for both ^{1}H and ^{13}C.This study demonstrates that scaled DFT/B3LYP calculations are a powerful approach for understanding the vibrational spectra of medium sized organic compounds.

References

1. "Diagnostic Criteria for Alcohol Abuse and Dependence - Alcohol Alert No. 30-1995".

2. Jump up to:[a] [b] Kahan, M. (Apr 1996). "Identifying and managing problem drinkers". *Can Fam Physician* 42: 661–71.

3. Mezler M., Müller T., Raming K. (February 2001). "Cloning and functional expression of GABA(B) receptors from Drosophila". *Eur. J. Neurosci.* 13 (3): 477–486.

4. Dzitoyeva S., Dimitrijevic N., Manev H. (April 2003). "Gamma-aminobutyric acid B receptor 1 mediates behavior-impairing actions of alcohol in Drosophila: adult RNA interference and pharmacological evidence". *Proc. Natl. Acad. Sci. U.S.A.* 100 (9): 5485–5490.

5. Bexis S., Phillis B. D., Ong J., White J. M., Irvine R. J. (2004-04-09). "Baclofen prevents MDMA-induced rise in core body temperature in rats". *Drug and Alcohol Dependence* 74 (1): 89–96.

6. A.D. Becke, J. Chem. Phys. 98 (1993) 5648–5652.

7. C. Lee, W. Yang, R.G. Parr, Phys. Rev. B 37 (1988) 785–789.

8. B. Miehlich, A. Savin, H. Stoll, H. Preuss, Chem. Phys. Lett. 157 (1989)200-206.

9. M.J. Frisch, G.W. Trucks, H.B. Schlegel et al., Gaussian 03, Revision A.1,Gaussian, Pittsburgh.PA.USA.2003.

10. M.J. Frisch, G.W. Trucks, H.B. Schlegel, G.E. Scuseria, M.A. Robb, J.R. Cheeseman,B. Johnson, W.M. Chen, W. Wong, C. Gonzalez, J.A. Pople, Gaussian, Inc.,Wallingford, CT, 2004.

11. H.B. Schlegel, J. Comput. Chem. 3 (1982) 214–218.

12. E.D. Glendening, A.E. Reed, J.E. Carpenter, F. Weinhold, NBO Version 3.1. TCI,University of Wisconsin, Madison, 1998.

13. A. Frish, A.B. Nielsen, A.J. Holder, Gauss View User Manual, Gaussian Inc.,Pittsburgh, PA, 2001.

14. Gaussian 03 Program, Gaussian Inc., Wallingford, CT, 2004.

15. I.H. Grebogi, A.U.V. Tibola, A. Barison, C.W.P.S. Grandizoli, H.G. Ferraz, L.N.C.

16. Rodrigues, J. Incl. Phenon. Marcocycl. Chem. 10 (1007) (2011) 3.

17. www.Chemcraft.com.

18. Bellamy L J 1980 The infrared spectra of complex molecules (London: Chapman and Hall) vol 2

19. A. Prabakaran, S. Muthu, Spectrochim. Acta A 99 (2012) 90–96.

20. Wiberg K B and Sharke A 1973 SpectrochimActa A29 583

21. V.K. Rastogi, M.A. Palafox, R.P. Tanwar, L. Mittal, Spectrochim. Acta A 58 (2002)1987– 2004.

22. M. Silverstein, G.C. Basseler, C. Morill, Spectrometric Identification of OrganicCompounds, Wiley, New York, 1981.

23. L.J. Bellamy, The Infrared Spectra of Complex Molecules, third ed., Wiley, NewYork, 1975.

24. L.J. Bellamy, The Infrared Spectra of Complex Molecules, third ed., Wiley, NewYork, 1975.

25. G. Varsanyi, Assignmnet of Vibrational Spectra of Seven Hundred BenzeneDerivatives, vols. 1–2, Adam Hilgler, 1974.

26. N.B. Colthup, L.H. Daly, S.E. Wiberley, Introduction to Infrared and RamanSpectroscopy, Academic Press, New York, 1990.

27. S. Muthu, E.I. Paulraj, Solid State Sci. 14 (2012) 476–487.

28. D. Sajan, J. Binoy, B. Pradeep, K.V. Krishna, V.B. Kartha, I.H. Joe, V.S. Jayakumar,Spectrochim. Acta A 60 (2004) 173–180.

29. GunasekaranS,Seshadri S &MuthuS,*Indian J Pure &Appl Phys,*43.503(2005)

30. Gunasekaran S ,Sankari G,&PonnusamyS,*Spectrochim Acta*,61A(2005)117

31. R. Meenakshi, Mol. Simulat. 36 (6) (2010) 425.

32. M. AlcoleaPalafox, Int. J. Quantum Chem. 77 (2000) 661–684.

33. X. Sun, Q.L. Hao, W.X. Wei, Z.X. Yu, D.D. Lu Wang, Y.S. Wang, Mol. Struct.THERMOCHEM. 74 (2009) 901–904.

34. P. Politzer, F.A. Awwad, Theor. Chem. Acc. 99 (1998) 83–87.

35. Y.X. Sun, Q.L. Hao, Z.X. Yu, W.X. Wei, L.D. Lu, X. Wang, Mol. Phys. 107 (2009)223.

36. A.B. Ahmed, H. Feki, Y. Abid, H. Boughzala, C. Minot, A. Mlayah, J. Mol. Struct.920 (2009)1.

37. J.P. Abraham, D. Sajan, V. Shettigar, S.M. Dharmaprakash, N.I.H. Joe, V.S.Jayakumar, J. Mol. Struct. (2009) 917–927.

38. S.G. Sagdinc, A. Esme, Spectrochim. Acta A 75 (2010) 1370–1376.

39. A.B. Ahamed, H. Feki, Y. Abid, H. Boughzala, C. Monit, Spectrochim. Acta A 75(2010) 293–298.

40. P. Pulay, G. Fogarasi, G. Ponger, J.E. Boggs, A. Vargha, J. Am. Chem. Soc. 105(1983) 7073–7078.

41. G. Fogarasi, X. Zhou, P.W. Taylor, P. Pulay, J. Am. Chem. Soc. 114 (1992) 8191–8201.

42. B.Osmialowski,E.Kolehmainen,R.Gawinencki,   Magn,Reson.chem.29(2001) 334-340

43. R.Marek,J.Brus, J.Tousk, L.kovacs,D.Hockova,Magn.Reson chem.40(2002)353-360

44. Vasanthy M and M. Jeganathan. 2007. Ambient air quality in terms of NOx in and around Ariyalur, Perambalur DT, Tamil Nadu. Jr. of Industrial pollution Control., 23(1):141-144.

45. Vasanthy. M ,A.Geetha, M. Jeganathan,and A.Anitha. 2007. A study on drinking water quality in Ariyalur area. J.Nature Environment and Pollution Technology. 8(1):253-256.

46. Ramanathan R ,M. Jeganathan, and T. Jeyakavitha. 2006. Impact of cement dust on azadirachtain dicaleaves – ameasure of air pollution in and Around Ariyalur. J. Industrial Pollution Control. 22 (2): 273-276.

47. Vasanthy M and M. Jeganathan. 2007. Ambient air quality in terms of NOx in and around Ariyalur, Perambalur DT, Tamil Nadu. Pollution Research., 27(1):165-167.

48. Vasanthy M and M. Jeganathan. 2008.Monitoring of air quality in terms of respirable particulate matter – A case study. Jr. of Industrial pollution Control.,24(1):53 - 55.

49. Vasanthy M, A.Geetha, M. Jeganathan, and M. Buvaneswari. 2008. Phytoremediation of aqueous dye solution using blue devil (Eichhornia crassipes). J. Current Science. 9 (2): 903-906.

50. Raajasubramanian D, P. Sundaramoorthy, L. Baskaran, K. Sankar Ganesh,   AL.A. Chidambaram and M. Jeganathan. 2011. Effect of cement dust pollution on germination and growth of groundnut (*Arachis hypogaea* L.). IRMJ-Ecology. International Multidisciplinary Research Journal 2011, 1/1:25-30 : ISSN: 2231-6302: Available Online: http://irjs.info/.

51. Raajasubramanian D, P. Sundaramoorthy, L. Baskaran, K. Sankar Ganesh,   AL.A. Chidambaram and M. Jeganathan. 2011. Cement dust pollution on growth and yield attributes of groundnut. (*Arachis hypogaea* L.). IRMJ-Ecology. International Multidisciplinary Research Journal 2011, 1/1:31-36.ISSN: 2231-6302. Available Online: http://irjs.info/

52. Jeganathan M, K. Sridhar and J.Abbas Mohaideen. 2012. Analysis of meterological conditions of Ariyalur and construction of wind roses for the period of 5 years from January 2002. J.Ecotoxicol.Environ.Monit., 22(4): 375-384.

53. Sridhar K, J.Abbas Mohaideen M. Jeganathan and P Jayakumar. 2012. Monitoring of air quality in terms of respirable particulate matter at Ariyalur, Tamilnadu. J.Ecotoxicol.Environ.Monit., 22(5): 401-406.

54. Jeganathan M, K Maharajan C Sivasubramaniyan and A Manisekar. 2014. Impact of cement dust pollution on floral morphology and chlorophyll of *healianthus annus* plant – a case study. J.Ecotoxicol.Environ.Monit., 24(1): 29-34.

55. Jeganathan M, C Sivasubramaniyan A Manisekar and M Vasanthy. 2014. Determination of cement kiln exhaust on air quality of ariyalur in terms of suspended particulate matter – a case study. IJPBA. 5(3): 1235-1243. ISSN:0976-3333.

56. Jeganathan M, S Gunaselvi K C Pazhani and M Vasanthy. 2014. Impact of cement dust pollution on floral morphology and chlorophyll of *healianthus annus*.plant a case study. IJPBA. 5(3): 1231-1234. ISSN:0976-3333.

57. Gunaselvi S, K C Pazhani and M. Jeganathan. 2014. Energy conservation and environmental management on uncertainty reduction in pollution by combustion of swirl burners. J. Ecotoxicol. Environ.Monit., 24(1): 1-11.

58. Jeganathan M, G Nageswari and M Vasanthy. 2014. A Survey of traditional medicinal plant of Ariyalur District in Tamilnadu. IJPBA. 5(3): 1244-1248. ISSN:0976-3333.

59. Premalatha P, C. Sivasubramanian, P Satheeshkumar, M. Jeganathan and M. Balakumari.2015. Effect of cement dust pollution on certain physical and biochemical parameters of castor plant (*ricinus communis*). IAJMR.1(2): 181-185.ISSN: 2454-1370.

60. Premalatha P, C. Sivasubramanian, P Satheeshkumar, M. Jeganathan and M. Balakumari.2015. Estimation of physico-chemical parameters on silver beach marine water of cuddalore district. Life Science Archives. 1(2): 196-199.ISSN: 2454-1354.

61. Seshadri V, C. Sivasubramanian P. Satheeshkumar M. Jeganathan and Balakumari.2015. Comparative macronutrient, micronutrient and biochemical constituents analysis of *arachis hypogaea.* IAJMR.1(2): 186-190.ISSN: 2454-1370.

62. Seshadri V, C. Sivasubramanian P. Satheeshkumar M. Jeganathan and Balakumari.2015. A detailed study on the effect of air pollution on certain physical and bio chemical parameters of <u>*mangifera indica*</u> plant.Life Science Archives. 1(2): 200-203.ISSN: 2454-1354.

63. Shakila N, C. Sivasubramanian, P. Satheeshkumar, M. Jeganathan and Balakumari.2015. Effect of municipal sewage water on soil chemical composition- A executive summary. IAJMR.1(2): 191-195.ISSN: 2454-1370.

64. Shakila N, C. Sivasubramanian, P. Satheeshkumar, M. Jeganathan and Balakumari.2015. Bacterial enumeration in surface and bottom waters of two different fresh water aquatic eco systems in Ariyalur, Tamillnadu. Life Science Archives. 1(2): 204-207.ISSN: 2454-1354.

65. Ashok J, S. Senthamil kumar, P. Satheesh kumar and M. Jeganathan. 2016. Analysis of meteorological conditions of ariyalur district. Life Science Archives. 2(3): 579-585.ISSN: 2454-1354. DOI: 10.21276/lsa.2016.2.3.9.

66. Ashok J, S. Senthamil Kumar, P. Satheesh Kumar and M. Jeganathan. 2016. Analysis of meteorological conditions of cuddalore district. IAJMR.2 (3): 603-608.ISSN: 2454-1370. DOI: 10.21276/iajmr.2016.2.3.3.

67. Satheesh Kumar P, C. Sivasubramanian, M. Jeganathan and J. Ashok. 2016. South Indian vernacular architecture -A executive summary. IAJMR.2 (4): 655-661.ISSN: 2454-1370. DOI: 10.21276/iajmr.2016.2.3.3.

68. Satheesh Kumar P, C. Sivasubramanian, M. Jeganathan and J. Ashok. 2016. Green buildings - A review. Life Science Archives. 2(3): 586-590.ISSN: 2454-1354. DOI: 10.21276/lsa.2016.2.3.9.

69. Satheesh Kumar P, C. Sivasubramanian, M. Jeganathan and J. Ashok. 2016. Indoor outdoor green plantation in buildings - A case study. IAJMR.2 (3): 649-654.ISSN: 2454-1370. DOI: 10.21276/iajmr.2016.2.3.3.

70. Manikandan R, M. Jeganathan, P. Satheesh Kumar and J. Ashok. 2016. Assessment of ground water quality in Cuddalore district, Tamilnadu, India. Life Science Archives. 2(4): 628-636.ISSN: 2454-1354. DOI: 10.21276/lsa.2016.2.3.9.

71. Manikandan R, M. Jeganathan, P. Satheesh Kumar and J. Ashok. 2016. A study on water quality assessment of Ariyalur district, Tamilnadu, India. IAJMR.2 (4): 687-692.ISSN: 2454-1370. DOI: 10.21276/iajmr.2016.2.3.3.

72. Sethuraman G, M. Jeganathan, P. Satheesh Kumar and J. Ashok. 2016. Assessment of air quality in Ariyalur, Tamilnadu, India. Life Science Archives. 2(4): 637-640.ISSN: 2454-1354. DOI: 10.21276/lsa.2016.2.3.9.

73. Sethuraman G, M. Jeganathan, P. Satheesh Kumar and J. Ashok. 2016. A study on air quality assessment of Neyveli, Tamilnadu, India. IAJMR.2 (4): 693-697.ISSN: 2454-1370. DOI: 10.21276/iajmr.2016.2.3.3.

74. Malarvannan J, C. Sivasubramanian, R. Sivasankar, M. Jeganathan and M. Balakumari. 2016. Shading of building as a preventive measure for passive cooling and energy conservation – A case study. Indo – Asian Journal of Multidisciplinary Research (IAJMR): ISSN: 2454-1370. Volume – 2; Issue - 6; Year – 2016; Page: 906 – 910. DOI: 10.21276.iajmr.2016.2.6.10.

75. Malarvannan J, C. Sivasubramanian, R. Sivasankar, M. Jeganathan and M. Balakumari. 2016. Assessment of water resource consumption in building construction in tamilnadu, India. Life Science Archives (LSA) ISSN: 2454-1354 Volume – 2; Issue - 6; Year – 2016; Page: 827 – 831 DOI: 10.21276/lsa.2016.2.6.7.

76. Sivasankar R, C. Sivasubramanian, J. Malarvannan, M. Jeganathan and M. Balakumari. 2016. A Study on water conservation aspects of green buildings. Life Science Archives (LSA),ISSN: 2454-1354. Volume – 2; Issue - 6; Year – 2016; Page: 832 – 836, DOI: 10.21276/lsa.2016.2.6.8.

77. Ashok J , S. Senthamil Kumar , P. Satheesh Kumar and M. Jeganathan. 2016. Analysis and design of heat resistant in building structures. Life Science Archives (LSA), ISSN: 2454-1354. Volume – 2; Issue - 6; Year – 2016; Page: 842 – 847. DOI: 10.21276/lsa.2016.2.6.10.